Industrial Crops & Products 230 (2025) 121094

Contents lists available at ScienceDirect

Industrial Crops & Products

journal homepage: www.elsevier.com/locate/indcrop

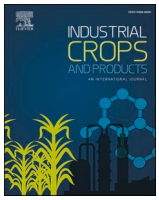

Waste from hemp essential oil production: How distillation methods shape the byproducts value

Eleonora Spinozzi [a,*], Luca Boldrini [a], Marta Ferrati [a], Erica Betti [a], Massimo Ricciutelli [a], Valtcho D. Zheljazkov [b], Stefano Dall'Acqua [c], Stefania Sut [c], Marco Cespi [a], Riccardo Petrelli [a], Filippo Maggi [a]

[a] Chemistry Interdisciplinary Project (ChIP) Research Center, School of Pharmacy, University of Camerino, Via Madonna delle carceri, Camerino 62032, Italy
[b] Crop and Soil Science Department, 3050 SW Campus Way, Oregon State University, Corvallis, OR 97331, USA
[c] Department of Pharmaceutical and Pharmacological Sciences, Natural Product Laboratory, University of Padova, Padova, Italy

ARTICLE INFO

Keywords:
CBD
Circular economy
Essential oil
Hemp

ABSTRACT

The valorization and reuse of waste products is a hot topic within the circular economy framework of industrial hemp (*Cannabis sativa* L.). The distillation of hemp biomass to produce the essential oil (EO) generates a notable amount of waste (spent biomass and residual water) worthy of reuse for the recovery of several bioactives, i.e., cannabinoids and polyphenols. Given this, it has been hypothesized that both the distillation method and its duration may influence the composition and yield of bioactive compounds from these byproducts. Thus, the aim of this study was to evaluate the effect of different techniques for the EO recovery [steam-distillation (SD), hydrodistillation (HD), and microwave-assisted hydrodistillation (MAH)] from the inflorescences of the monoecious cv. Felina 32 combined with different distillation times (60, 120, 240, 360, and 480 min) on: (i) cannabinoids content in spent biomass extracted through supercritical fluid extraction (SFE), (ii) phenolic compounds in lyophilized residual water. All distillation techniques and durations were effective for the decarboxylation of cannabinoid acids in the residual biomass with the consequent formation of their neutral forms (mainly CBD) in high amounts. The residual water was found to be enriched in luteolin and apigenin derivatives. Hence, this work demonstrated that different distillation techniques and durations for hemp EO production can yield valuable residual byproducts (spent biomass and residual water) suitable for further industrial applications.

1. Introduction

Industrial hemp (*Cannabis sativa* L., Cannabaceae) is a versatile crop known for its sustainable and eco-friendly cultivation (Struik et al., 2000). The recent legalization of hemp in many countries has significantly boosted its industrial use, fueled by expanded acreage, a growing global market, and the discovery of new applications. These applications span a wide range of sectors, from energy and sustainable materials to food, health, and wellness, highlighting the potential of hemp as a versatile and valuable crop. The wide array of valuable products derived from hemp across various sectors makes it especially well-suited for the circular economy, aligning with zero-waste management principles for crops and their by-products. This versatility enhances the potential of hemp as a sustainable resource within environmentally-friendly production systems.

Among the many hemp-derived products utilized in industry, essential oil (EO), a traditional distillation product from plant inflorescences rich in volatile terpenes, has garnered significant attention. Its diverse biological properties, including antimicrobial, insecticidal, acaricidal, anti-inflammatory, antinociceptive, analgesic, anticonvulsant, and neuroprotective effects, make hemp EO particularly valuable for many applications (Benelli et al., 2018a; Nuutinen, 2018; Rossi et al., 2020; Tabari et al., 2020; Zheljazkov et al., 2020a; Laws and Smid, 2022; Barbalace et al., 2023; Schwarz et al., 2023). Consequently, it finds application in pharmaceutical, cosmetic, perfumery, and agrochemical fields (Mazzara et al., 2023). Hemp EO is composed of three main chemical classes of compounds, namely monoterpenes, sesquiterpenes, and cannabinoids (Fiorini et al., 2019). The EO yield and chemical

* Corresponding author.
E-mail address: eleonora.spinozzi@unicam.it (E. Spinozzi).

https://doi.org/10.1016/j.indcrop.2025.121094
Received 4 February 2025; Received in revised form 20 April 2025; Accepted 22 April 2025
Available online 30 April 2025

profile can vary significantly, influenced primarily by factors such as the hemp cultivar, storage conditions, processing methods, and distillation techniques (Dudziec et al., 2024).

During hemp inflorescences distillation a significant amount of waste material is generated, including residual water (distillation wastewater) and depleted biomass (spent material from distillation). These byproducts, accounting for approximately 99% of the initial biomass, hold significant potential within the circular economy framework, being still rich in valuable recoverable compounds (Mazzara et al., 2022a).

The residual water is generally rich in phenolic compounds, including luteolin and apigenin derivatives, with cannflavins being the most investigated for their anti-inflammatory, neuroprotective, anticancer, and antiparasitic activity (Erridge et al., 2020; Gunjevic et al., 2021; Izzo et al., 2020; Mazzara et al., 2022b). The spent biomass, composed of depleted inflorescences, remains valuable for the recovery of bioactive compounds, primarily cannabinoids (Mazzara et al., 2022a). Zheljazkov and Maggi (2021) have shown that when hemp inflorescences are left unchopped and subjected to steam distillation, the glandular trichomes responsible for the synthesis and storage of plant secondary metabolites, remain intact, losing only volatile compounds through evaporation. In this state, less volatile and non-volatile compounds, such as cannabinoids, are retained within the glandular trichomes without chemical degradation. Furthermore, the same authors demonstrated that a 240-minute steam distillation induces decarboxylation reactions in the residual biomass, thereby increasing the content of pharmacologically active neutral cannabinoid forms. This finding has also been corroborated by other authors as well (Gunjevic et al., 2021). Therefore, distillation can also be viewed as an intermediate process in the manufacturing of cannabinoid-rich extracts, avoiding the need for additional decarboxylation steps typically required to convert the acidic forms into their neutral counterparts before the extraction.

Although the study by Zheljazkov and Maggi (2021) provided new insights into how distillation can enhance cannabinoid content in distilled biomass without requiring decarboxylation, there is, to our knowledge, no data on how different distillation techniques and conditions affect this process. In this study, we compared and evaluated the effect of three techniques for the EO distillation [steam-distillation (SD), hydrodistillation (HD), and microwave-assisted hydrodistillation (MAH)] carried out at various distillation times (from 60 to 480 min) on the cannabinoids content in the depleted biomass and phenolic compounds content in the residual water. Regarding cannabinoids recovery, a green extraction method using supercritical CO_2 was developed and optimized. This research aimed to develop a near zero-waste management approach to produce different hemp bioactives for multiple applications.

2. Materials and methods

2.1. Chemicals and reagents

Cannabidivarin (CBDV), cannabidiol (CBD), cannabigerol (CBG), cannabidiol acid (CBDA), and cannabichromene (CBC) employed for the HPLC-DAD quantitative analysis were purchased from Supelco (Bellefonte, USA). HPLC-grade acetonitrile and methanol employed for the HPLC-DAD analysis, as well as formic acid (99%), were purchased from Merck (Milan, Italy). Deionized water (>18 MΩ cm resistivity) was further purified through a Milli-Q SP Reagent Water system (Millipore, Bedford, MA, USA). All the solvents and solutions for HPLC-DAD analysis were filtered through a polyamide syringeless filter (0.2 μm) (Sartorius Stedim, Goettingen, Germany). *n*-Hexane employed for the GC-MS analysis was purchased from Carlo Erba (Italy). The mix of C_7–C_{40} alkanes, as well as standards and reagents employed for the spectrophotometric assays were acquired from Merck (Milan, Italy).

2.2. Plant material

The inflorescences of the monoecious cv. Felina 32 were collected from a cultivation in Fiuminata, Marche, Italy (GPS coordinates N 43°11'11", E 12°56'24", 318 m a.s.l.) on 29 July 2022. The seedlings were grown by the farm La Biologica Società Cooperativa Agricola. An herbarium specimen was identified by F. Maggi according to the Italian Flora (Pignatti, 1982) and archived in the *Herbarium Camerinensis* of the School of Bioscience and Veterinary Medicine (University of Camerino) under the codex CAME#29332. Immediately after collection, the plant material was transported to the Chemistry Interdisciplinary Project (ChIP) Research Center at the University of Camerino and stored at –20°C until further use. Freezing was selected as a conservative storage method to prevent oxidative reactions, minimize terpene loss, and preserve the antioxidant activity and phenolic compounds in the biomass (Chen and Pan, 2021). The term "fresh samples" used throughout the manuscript refers to the thawed samples. The moisture content was determined on three samples of randomly-collected frozen inflorescences after heating at 100°C in a thermobalance (Scaltec SMO 01, Scaltec instruments GmbH, Heiligenstadt, DE). The average moisture content of the biomass was 73 ± 1.1%.

2.3. Distillation of the essential oil (EO)

The volatile fraction of hemp was obtained through the techniques outlined below, that were performed on fresh hemp inflorescences (500 g) with different distillation durations: 60, 120, 240, 360, and 480 min. Each distillation was performed twice and the EOs, of a pale-yellow color, were collected, dried with anhydrous Na_2SO_4, and stored at 4°C until chemical analysis. The EO yield was expressed as g of EO obtained from 100 g of dry inflorescences ($\%_{DW}$).

2.3.1. Hydrodistillation (HD)

Hemp inflorescences were inserted into a 10- L round bottom flask filled with 5 L of deionized water. The system was heated using a Falc MA mantle (Falc Instruments, Treviglio, Italy) and the EO was collected with a Clevenger apparatus at different distillation times, as mentioned in Section 2.3.

2.3.2. Steam distillation (SD)

The inflorescences were subjected to steam distillation (SD) using an Albrigi Luigi E0106 (Stallavena di Grezzana-Verona, Italy) stainless steel apparatus (capacity of 20 L) for different distillation times, as mentioned in Section 2.3. The steam was generated from 2 L of deionized water placed at the bottom of the apparatus.

2.3.3. Microwave-assisted hydrodistillation (MAH)

The MAH was performed using an advanced microwave extraction system (ETHOS X, Milestone, Sorisole, Italy). The instrument was composed of a microwave reactor of 2.45 GHz, consisting of an infrared sensor monitoring the temperature and two magnetrons with a maximum delivery power of 1800 W (2 × 900 W). All runs were carried out using a 5- L glass reactor (Pyrex) with a glass cover working at atmospheric pressure. The system was equipped with a Clevenger-type apparatus above the oven, made of stainless steel ('Fragrances set-up'). Additionally, a Chiller Smart H150–2100S from Labtech Srl (Sorisole, Bergamo, Italy) was used to maintain the cooling water temperature at 8°C. The conditions chosen derived from a previously published work (Mazzara et al., 2022b): i.e., microwave power of 1.77 W/g of fresh inflorescences and water added to the material of 31.5% of the total weight loaded into the extractor. The MAH runs were performed with different distillation times, as reported in Section 2.3.

2.4. Essential oils (EOs) analysis

For both GC-MS and GC-FID analyses, the EOs were diluted (1:100)

in *n*-hexane, and 1 μL was injected in split mode (1:200 and 1:100 for the GC-MS and the GC-FID analysis, respectively). The characterization of EOs was performed through an Agilent 8890 GC-MS. The detector was a single quadrupole, model 5977B, purchased from Agilent (Santa Clara, California, USA). The instrument was equipped with an autosampler PAL RTC120 (CTC Analytics AG, Zwingen, Switzerland). The molecules, after separation in an HP-5MS capillary column (30 m l., 250 μm i.d., 0.25 μm f.t.), were ionized by utilizing an electron ionization source (EI).

The GC-FID analysis was performed using an Agilent 8890 gas chromatograph (GC) coupled to an ionization flame detector (FID) and equipped with an autosampler 7693 A from Agilent. The injector temperature was set at 250°C, and He served as the carrier gas at a flow rate of 1.28 mL/min. The separation of compounds was achieved on an HP-5MS capillary column (30 m l., 320 μm i.d., 0.25 μm f.t.). The column temperature was set at 60°C for 5 min, then increased to 220°C at a rate of 4 °C/min, followed by a ramp to 280°C at 11 °C/min, held for 15 min, and finally elevated to 300°C at 15 °C/min and held for 0.5 min. The total run time was approximately 67 min. The FID heater was set at 250°C, H_2 flow was set at 30 mL/min, and air flow was 400 mL/min. The chromatograms were analyzed using the Agilent OpenLab CDS ChemStation Edition (Agilent, Santa Clara, California, United States). Compound identification was obtained through a comparison with the MS fragmentation and then it was confirmed by calculation of the temperature-programmed retention index (RI). According to the Van Den Dool and Kratz. (1963) formula, the RI was calculated using the mixture of *n*-alkanes (C_7-C_{40}). Semi-quantification of the EO compounds was performed by using the same analytical conditions as those reported by Gugliuzzo et al. (2023).

2.5. Byproducts processing

2.5.1. Supercritical fluid extraction (SFE) of depleted hemp biomass

The depleted biomass collected after the distillation was dried at 40°C for 16 h through a Biosec desiccator (Tauro Essiccatori, Vanzo Nuovo, Vicenza, Italy). Then, the biomass was stored at room temperature, protected from light, and shredded to 1.5 mm particle-size employing a shredder (Albrigi, mod. E0585, Stallavena, Verona Italy) right before undergoing SFE. The major cannabinoids were extracted with a Supercritical Fluid Extractor SFT-120XW (Supercritical Fluid Technologies, Inc.) consisting of an extraction chamber of 100 mL and operating at pressures up to 10,000 psi (68.9 MPa) and temperatures ranging from r.t. to 200°C. The system allows the use of ethanol as co-solvent. The employed supercritical fluid was liquid CO_2 whose flow was regulated by the SFT-Nex10 pump (Supercritical Fluid Technologies, Inc.). The system operated in two different modes: a static mode, in which a fixed volume of supercritical fluid is used inside the extraction chamber and a dynamic mode, where new supercritical fluid flows continuously through the pressure vessel. The SFE extract is generally collected in EPA vials. The extraction was performed on approximately 10 g of depleted powdered dry biomass. In the trials with the co-solvent, ethanol was employed (20 mL). This process was performed prior to the flow of CO_2 inside the extraction chamber. The SFE yield was calculated as g of SFE extract from 100 g of dry depleted biomass ($\%_{DW}$). Once collected, the SFE extract was stored at 4°C until chemical analysis.

The optimal conditions for SFE were determined through a design of experiments (DoE) approach. The parameters that potentially influence the SFE process, namely temperature, pressure, extraction time, co-solvent, and cycles, were identified in a preliminary screening step using a 2-level half fractional factorial design (FFD) (Lewis et al., 1999). The selected FFD required 16 experimental runs and was characterized by a resolution of V (Lewis et al., 1999), which provides an excellent compromise for a screening design, allowing for nearly independent estimation of the main effects and 2-factor interactions (Lewis et al., 1999). The complete list of all 16 extraction runs, along with the corresponding coded and uncoded variables, are presented in Table S1 (Supplementary material). Each extraction run was characterized in terms of SFE yield, and the results were analyzed using a multilinear regression model that includes linear and 2-factor interaction terms, suitable for a resolution V design:

$$y = \beta_0 + \sum_{i=1}^{n} \beta_i \cdot x_i + \sum_{i<j}^{n} \beta_{ij} \cdot x_i x_j \quad (1)$$

where, y represents the response variable (yield), while β_0, β_i, and β_{ij} are the model constant, the coefficients corresponding to the linear terms x_i, and the coefficients for the first-order interaction terms $x_i x_j$, respectively.

A multilinear regression analysis was conducted using a stepwise procedure (backward elimination) to refine the model variables. The most appropriate model for yield was identified by comparing all generated models based on the adjusted coefficient of multiple determination (R^2_{adj}) and Mallows' *Cp* statistic. The selected model was evaluated through ANOVA, as well as coefficient and residual analysis. Following the FFD results, the cycle parameter was further analyzed using a CCD. In the FFD, the cycle parameters were set at two levels: some runs were conducted with no cycles (static conditions throughout the entire extraction), while others were run applying 3 cycles with a static/dynamic ratio of 2.33 (70% of each cycle was in static mode, and 30% in dynamic mode). The CCD was selected to independently examine the effect of the number of cycles and the static/dynamic ratio. The experimental domain of interest ranged from 1 to 5 cycles and from 90 to 50% static time relative to the total extraction time (corresponding to a static/dynamic ratio of 9–1). The effect of the number of cycles and static time percentage was analyzed using a two-factor CCD, comprising four factorial experiments (2^2), four axial experiments (2×2), and two replicates of the central experiments. The axial points were set with a α value of 2, instead of the standard 1.41 (the rationale for this choice is detailed in the Supplementary material, Section 1.1.2). According to Draper and Pukelsheim (1990), an α value of 2 in a two-factor CCD has a minor impact on design rotatability. All ten extractions were performed by varying the number of cycles and static time percentage as outlined in Table 1, and setting the pressure, temperature, and extraction time at 50 MPa, 70°C, and 50 min, respectively, without the use of a co-solvent.

Table 1
Runs for the Central Composite Design (CCD) for supercritical fluid extraction (SFE) of hemp depleted biomass.

		Uncoded variables		Coded variables	
Runs	**Point type**[a]	**Cycles (N°)**	**Static-dinamic ratio (%)**	**Cycles (N°)**	**Static-dinamic ratio (%)**
1	A	2	60	−1	−1
2	A	4	60	+1	−1
3	A	2	80	−1	+1
4	A	4	80	+1	+1
5	F	1	70	−2	0
6	F	5	70	+2	0
7	F	3	50	0	−2
8	F	3	90	0	+2
9	C	3	70	0	0
10	C	3	70	0	0

[a] The point type defines if certain experimental conditions represent a factorial (F), axial (A), central (C) point in the experimental domain of CCD.

For each extraction (Table 1), the yield was determined as described in Section 2.6, and its relationship with the CCD parameters was evaluated using multilinear regression with a full quadratic model:

$$y = \beta_0 + \sum_{i=1}^{n} \beta_i \cdot x_i + \sum_{i=1}^{n} \beta_{ii} \cdot x_i^2 \sum_{i<j}^{n} \beta_{ij} \cdot x_i x_j$$

where, y, β_0, β_i, and β_{ij} have the same meaning as in the Eq. 1, while β_{ii} are the coefficients of the quadratic terms x_i^2.

A multilinear regression analysis was performed using a stepwise (backward elimination) approach to refine the model variables. The

most suitable model for yield was determined by comparing all generated models based on the R^2_{adj}, on the predicted coefficient of multiple determination (R^2_{pred}) and Mallows' Cp statistic. The most suitable model was then evaluated by ANOVA, along with coefficient and residual analyses. The design and analysis of the DoE were performed using Minitab 18.

2.5.2. Residual water processing

The residual water in the reactor deriving from each distillation was collected and filtered, frozen using liquid nitrogen, and freeze-dried with a BUCHI Lyovapor™ L-200 freeze-dryer (Büchi Labortechnik AG, Flawil, Switzerland) operating at −50°C and 0.07 mbar. The lyophilized product was expressed as dry extract (DE).

2.6. Analysis of SFE extracts and residual water

2.6.1. HPLC-DAD analysis of SFE extracts

2.6.1.1. Stock solutions preparation. Cannabinoids (CBDV, CBD, CBG, CBDA, and CBC) were diluted in methanol at 1000 μg mL^{-1}. THC was quantified employing the calibration curve of CBD. The SFE extracts were diluted at 1000 μg mL^{-1} in methanol/acetonitrile (75:25, v/v). Before HPLC-DAD analysis, the standards and the SFE extracts were mixed vigorously with the help of a vortex for about 1 min and then further put in the ultrasound bath for about 5 min. Finally, they were filtered using a 0.2 μm syringeless filter.

2.6.1.2. HPLC-DAD analytical conditions. The HPLC was an Agilent 1100 series (Agilent Technologies, Santa Clara, CA, USA), consisting of a binary solvent pump, an autosampler, and a photodiode array detector (DAD), controlled by ChemStation (Agilent, v.01.03). The chromatographic separation was carried out on a Kinetex C18 (4.6 ×150 mm, particle size 2.6 μm), purchased from Phenomenex (Chesire, UK), operating at 35°C. The analysis was conducted with a mobile phase consisting of two solvents: water (A) and acetonitrile/methanol (75/25, v/v) (B) both added with 0.1% of formic acid. A linear gradient starting with 80% B was set to reach 100% B at 10 min, held for 15.50 min, and then the column was reconditioned for 15 min. The flow rate was 1 mL/min and the injection volume was 1 μL. The chromatograms were recorded at 210, 220, and 228 nm, accordingly to the maximum absorption of the analytes. In detail, 210 nm was the wavelength employed for the quantification of CBDV, CBD, THC, and CBG, while 220 nm for CBDA, and 228 nm for CBC.

2.6.1.3. Method validation. CBDV, CBD, CBG, CBDA, and CBC were confirmed using the analytical standards and calibration curves for quantitative purposes were obtained by injecting different concentrations of analyte standard solutions. In detail, the concentrations were 1, 3, 5, 10, 25, 50, 75, 100, 150, 200, and 400 ppm. The HPLC-DAD method was validated in terms of linearity, repeatability, limit of detection (LOD) and limit of quantification (LOQ) (Table S2, Supplementary material). The method linearity was determined by analyzing different concentrations of the analyzed cannabinoids (CBD, CBDV, CBD, CBG, CBDA, and CBG) (1, 3, 5, 10, 25, 50, 75, 100, 150, 200, and 400 ppm) and determining the coefficient of determination (R^2) (Figure S1, Supplementary material). The repeatability was assessed by determining the relative standard deviation (%RSD) between consecutive analyses (n = 5) performed in the same day (intraday reproducibility) and during 5 consecutive days (interday reproducibility). The LOD and LOQ were experimentally estimated by injecting low concentrations of the analyte standard solutions and measuring the signal-to-noise (S/N) ratio. A concentration giving a S/N ratio (height of peak/height of noise) of three was assigned to LOD while that of ten was assigned to LOQ (Table S2, Supplementary material).

2.6.2. HPLC-DAD-MS analysis of residual water

For the analysis of phytoconstituents in hemp DEs deriving from the three distillation techniques, a system formed by an Agilent 1260 chromatograph equipped with a diode array detector and coupled with a mass spectrometer ion trap Varian MS 500 using an electrospray ion source was employed. The column was an Agilent XDB C18 (3.0 ×150 mm, 3.5 μm) and the mobile phase consisted of water with 1% of formic acid (A) and acetonitrile (B). The gradient started with 5% of the organic phase (B) and increased to 100% in 30 min, the flow rate was 400 μL/min. The mass spectrometer operated in negative ion mode and data were acquired by Turbo Data Detecting Scan mode of the instrument that allows the generation of fragmentation scheme for compounds reaching a selected level of ion intensity. Compounds were identified based on their fragmentation pattern and comparison with the literature or reference compounds (Table S3, Supplementary material). Vitexin, rutin, cannflavin B, and caffeic acid (Merck, Milan, Italy) were used as reference standards for the quantification of *C*-glycosylated flavonoids, *O*-glycosylated flavonoids, cannflavins, and phenolic compounds, respectively. Each compound was solubilized in methanol, at a concentration of 50 μg/mL, and the solution was then diluted in methanol in order to obtain calibration curves as follows: $y = 29708x + 72240$, $R^2 = 0.9883$ for vitexin, $y = 44063x + 133815$, $R^2 = 0.9994$ for rutin, $y = 42011x + 37044$, $R^2 = 0.998$ for cannflavin B, $y = 6225.8x + 42157$, $R^2 = 0.9992$ for caffeic acid. For the analysis 200 mg of DE were extracted with 5 mL of methanol and sonicated for 20 min; supernatants were transferred in Eppendorf tubes, which were then centrifuged, filtered, and used for analysis.

2.7. Statistical analysis

The analysis of the distillation yield, as well as the cannabinoid yield from the depleted hemp biomass, was performed using two-way ANOVA at a 5% significance level. If necessary, post-hoc Tukey tests were conducted at a 5% family-wise significance level. The two-way ANOVA was conducted using the general linear model (GLM) approach with Minitab® 18.1 software (Minitab INC., USA). Pearson correlation analysis was carried out at a 5% significance level using Prism 6.01 software (GraphPad Inc., USA). When correlation coefficients (r) were found to be statistically significant, their strength was categorized based on absolute values as follows: $r \geq 0.9$ indicated a very strong correlation; values between 0.7 and 0.89 represented a strong correlation; those from 0.4 to 0.69 were considered moderate; correlations between 0.1 and 0.39 were classified as weak, while values equal or below 0.09 were regarded as negligible (Schober et al., 2018). A principal component analysis (PCA) was conducted using Minitab V18.1 (Minitab Inc., USA) to provide a general assessment of the impact of distillation techniques and time on the chemical composition of EO, residual water DE, and SFE extract. The PCA was performed in covariance mode when many components were present, which emphasizes variables with higher variances. On the other hand, a correlation matrix was utilized when the number of components was limited, ensuring that all variables were weighed equally by standardizing their scales.

3. Results and discussion

3.1. Essential oil (EO) distillation and chemical analysis

The differences between HD, SD, and MAH techniques are primarily linked to the type of heating. In SD the plant material is separated from the boiling water through a grid, while vapor, generated by a heating surface, passes through the plant material taking away all volatile compounds. These compounds are then condensed in the upper part of the system, which consists of a Clevenger-type apparatus and a collecting burette. In HD, water and plant material are placed together in the same reactor, with the boiling water coming into direct contact with the secretory structures. This process causes the evaporation of volatile

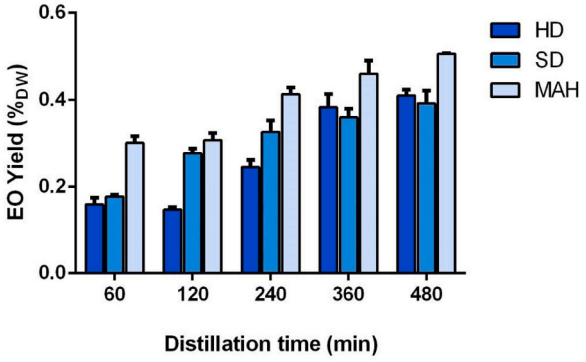

Fig. 1. Essential oil (EO) yields obtained with different distillation techniques (HD, hydrodistillation; SD, steam distillation, and MAH, microwave-assisted hydrodistillation) and distillation times (60, 120, 240, 360, and 480 min).

constituents and also promotes more aggressive hydrolytic and oxidative reactions in the biomass. The volatiles are then condensed and collected in the same way described as for SD. In both SD and HD, heating is generated by convection from the outside inward. Conversely, in MAH, the electromagnetic field generated by microwaves induces vibration of water molecules and other polar compounds within the vacuoles and secretory structures of plant cells. This leads to rapid increase in temperature and pressure. This process disrupts cell walls, leading to the release of metabolites (Filly et al., 2014). Among the compounds, the volatile ones are immediately vaporized and recovered by the same system used in SD and HD (Clevenger-type apparatus). Notably, in MAH, heating is volumetrically dissipated from the inside outward, enhancing the efficiency of the distillation process.

The EOs were obtained with diverse yields depending on the distillation technique and distillation time (0.15–0.41%$_{DW}$ for HD, 0.18–0.39%$_{DW}$ for SD, and 0.30–0.51%$_{DW}$ for MAH) (Fig. 1 and Tables S4, S5, and S6 Supplementary material). Generally, the EO yields obtained in this study were consistent with those previously reported for the same hemp cultivar (cv. Felina 32) and distillation techniques (Benelli et al., 2018a; Kavallieratos et al., 2020).

Analysis of variance (two-way ANOVA) identified time and distillation technique as statistically significant on the EO yields, with time having the greatest effect (Supplementary material, Figure S2). Additionally, the interaction between time and distillation techniques was also statistically significant, showing that the efficiency of HD was more time-dependent when compared with the others (Supplementary Figure S3). Post hoc Tukey's test showed that differences in EO yields between the three methods were all statistically significant, following the order: MAH > SD > HD. The greater efficiency of MAH compared to the other two conventional techniques has been already reported in literature (Fiorini et al., 2020; Gunjevicć et al., 2021), and more details are furnished in Section 2.1 of the Supplementary material.

As regards the GC-FID and GC-MS analyses, the hemp volatile constituents were identified as total percentages always higher than 92% of the total composition (Table 2). The major chemical classes of hemp EOs obtained by HD, SD, and MAH were monoterpene hydrocarbons (16.41–46.30%), sesquiterpene hydrocarbons (37.08–53.56%), cannabinoids (2.82–25.65%), and oxygenated sesquiterpenes (4.56–10.39%), while oxygenated monoterpenes were minor compounds (Table 2). The detailed chemical compositions are reported in Tables S4, S5, S6 (Supplementary material). The most representative compounds of these classes were α-pinene (3.56-13.69%), myrcene (4.71-11.61%), terpinolene (3.25-6.59%), (*E*)-caryophyllene (20.16-28.62%), and α-humulene (10.11-13.97%), CBD (3.78-20.85%), and caryophyllene oxide (3.25-5.92%), respectively (Tables S4, S5, S6). Concerning EOs obtained through HD, the relative percentages of the primary chemical groups in the EOs shifted with distillation time. Initially, at 60 min, monoterpene hydrocarbons (44.31%) were more abundant than sesquiterpenes

Table 2
Main monoterpene hydrocarbons, sesquiterpene hydrocarbons, oxygenated sesquiterpenes, and cannabinoids found in the essential oils (EOs) obtained by the three distillation techniques at different times (60, 120, 240, 360, and 480 min). The complete chemical compositions are reported in the Supplementary information.

	Area %[d]														
	HD					SD					MAH				
Compound[a]	**60**[e]	**120**	**240**	**360**	**480**	**60**	**120**	**240**	**360**	**480**	**60**	**120**	**240**	**360**	**480**
α-pinene	13.69	9.83	4.16	3.56	4.79	14.76	11.91	8.78	6.65	5.09	17.97	15.50	13.97	14.13	12.77
β-pinene	5.35	4.23	2.31	1.83	2.26	5.31	4.44	3.28	2.73	2.19	5.58	5.01	4.51	4.47	3.94
myrcene	11.61	9.32	5.74	4.71	5.46	11.09	9.12	7.38	6.29	5.42	11.23	9.92	9.57	9.22	8.06
(*E*)-β-ocimene	3.65	2.63	2.02	1.72	2.08	3.46	2.97	2.45	2.01	2.02	3.27	2.44	2.34	2.77	2.48
terpinolene	6.59	4.80	3.71	3.25	3.82	5.90	4.97	4.27	3.72	3.76	5.29	3.84	4.13	4.74	4.16
(*E*)-caryophyllene	20.16	22.99	26.66	28.62	24.71	19.41	21.78	21.45	22.49	22.04	21.05	22.33	22.27	21.66	19.71
α-humulene	10.11	11.71	13.30	13.97	12.18	10.09	10.82	10.64	11.18	10.85	10.30	11.05	10.88	10.62	9.40
caryophyllene oxide	5.08	5.92	5.48	3.96	3.25	4.30	4.41	4.63	3.93	2.93	3.12	4.57	3.91	2.90	2.48
cannabidiol	3.78	5.35	12.14	15.87	20.85	3.10	7.19	13.94	17.32	23.77	2.57	3.11	6.52	8.31	16.83
total of identifies compounds (%)	95.00	93.96	93.28	93.59	94.93	94.10	94.21	93.64	93.21	93.93	94.74	92.61	93.75	93.60	93.81
monoterpene hydrocarbons	44.31	33.48	19.67	16.41	20.02	43.77	36.19	28.29	23.31	20.18	46.30	39.27	37.08	37.88	33.64
oxygenated monoterpenes	0.30	0.30	0.23	0.12	0.14	0.55	0.67	0.78	0.96	0.97	0.10	0.14	0.15	0.09	0.12
sesquiterpene hydrocarbons	37.39	44.04	50.63	53.65	46.26	38.87	41.75	41.28	43.06	41.83	40.03	42.77	42.43	41.19	37.08
oxygenated sesquiterpenes	8.89	10.39	9.91	6.39	6.13	7.48	7.75	8.15	7.04	5.30	5.49	6.86	6.90	5.31	4.56
cannabinoids	4.12	5.74	12.84	17.01	22.38	3.42	7.86	15.15	18.85	25.65	2.82	3.57	7.19	9.13	18.41

[a]Components are ordered according to their elution from the HP-5MS column.
[b]Linear retention index calculated according to the Van den Dool and Kratz formula.
[c]Retention index taken from Adams.
[d]Relative percentage values are mean of two independent analyses.
[e]HD, hydrodistillation at 60, 120, 240, 360, and 480 min.

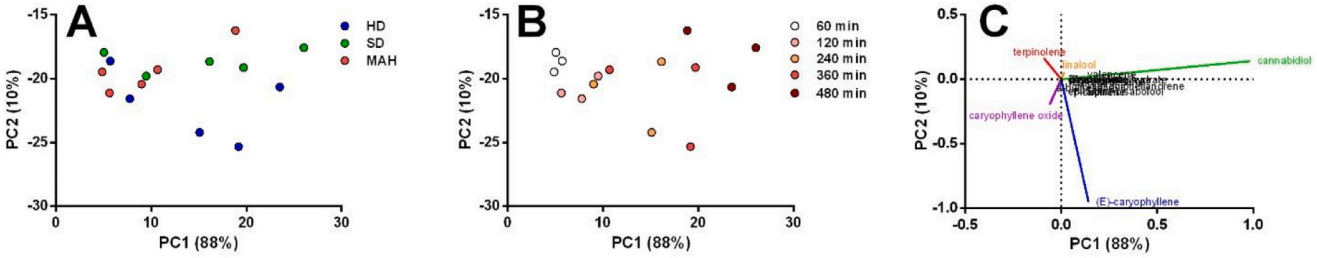

Fig. 2. PCA analysis performed on the essential oils (EOs) chemical compositions deriving from different techniques (A) (HD, hydrodistillation; SD, steam distillation, and MAH, microwave-assisted hydrodistillation) and distillation times (B) (60, 120, 240, 360, and 480 min).

(37.39%). However, beyond this point, sesquiterpenes became the dominant group over monoterpenes across all distillation times, with levels measured at 44.04% versus 33.48% at 120 min, 50.63% versus 19.67% at 240 min, 53.65% versus 16.41% at 360 min, and 46.26% versus 20.02% at 480 min. This trend suggests that prolonged distillation favors the concentration of sesquiterpenes. A similar trend was observed with cannabinoids, which were initially a minor fraction in the EO collected at 60 min (4.12%) but increased significantly to become the second most abundant group by 480 min (22.38%). This shift may be attributed to an increase in decarboxylative reactions within the plant matrix as distillation time progresses, converting cannabinoid acids into their neutral forms and thereby enhancing their presence in the EO (Tables S4, S5, S6, Supplementary material). Finally, oxygenated sesquiterpenes were rather consistent up to 240 min (8.89, 10.39, and 9.91% at 60, 120 and 240 min, respectively), and after that, they decreased up to 6.13%. A similar profile was observed in the EOs obtained by SD, with monoterpene hydrocarbons (20.18-43.77%), sesquiterpene hydrocarbons (38.87-43.06%), cannabinoids (3.42-25.65%), and oxygenated sesquiterpenes (5.30-8.15%) representing the main chemical groups (Tables S4, S5, S6). An opposite trend was observed between monoterpene hydrocarbons, which decreased from 43.77% at 60 min to 20.18% at 480 min, and cannabinoids, which increased from 3.42 to 25.65% over the same period. α-Pinene (5.09-14.76%), myrcene (5.42-11.09%), and terpinolene (3.72-5.90%), (*E*)-caryophyllene (19.41-22.49%) and α-humulene (10.09-11.18%), CBD (3.10-23.77%), and caryophyllene oxide (2.93-4.63%) were the most representative compounds of the main chemical groups (Tables S4, S5, S6). In the EOs obtained by MAH, a similar trend was observed: monoterpene hydrocarbons decreased from 46.30% at 60 min to 33.64% at 480 min, while cannabinoids increased from 2.82 to 18.41% over the same time period. In contrast, the percentages of sesquiterpene hydrocarbons (40.03% at 60 min to 37.08% at 480 min) and oxygenated sesquiterpenes (5.49% at 60 min to 4.56% at 480 min) remained relatively consistent throughout the distillation process. The major EO constituents once again were (in decrescent order of abundance) (*E*)-caryophyllene (19.71-22.33%), α-pinene (12.77-17.97%), CBD (2.57-16.83%), myrcene (8.06-11.23%), α-humulene (9.40-11.05%), terpinolene (3.84-5.29%), and caryophyllene oxide (2.48-4.57%). Generally, the chemical composition found in this study for all the EOs was similar to those reported by other authors for the cv. Felina 32. Indeed, the EO obtained from this cv. was mainly dominated by monoterpene hydrocarbons (54.0%) and sesquiterpene hydrocarbons (44.2%) (Benelli et al., 2018a). In detail, (*E*)-caryophyllene (23.8%), α-pinene (16.4%), and myrcene (14.2%) were the most abundant compounds, followed by terpinolene (9.6%), α-humulene (8.3%), β-pinene (5.2%), (*E*)-β-ocimene (5.1%), and (*E*)-β-farnesene (3.0%) (Benelli et al., 2018a). In contrast to the findings reported by Benelli et al. (2018a), where cannabinoids were almost absent, their levels in this study were notably high ranging from 4.12 to 22.38% in HD, 3.42 to 25.65% in SD, and 2.82 to 18.41% in MAH. The chemical composition reported in our study aligns linearly with the findings reported by Bertoli et al. (2010) for the cv. Felina 34. In their study, α-pinene (20.3–20.4%), (*E*)-caryophyllene (19.4–19.5%), terpinolene (15.0–19.1%), and myrcene (12.3–13.6%) were the major EO compounds (Bertoli et al., 2010). Regarding cannabinoids, the CBD content (1.39-13.85%) reported by Bertoli et al. (2010) was higher than that observed by Benelli et al. (2018b). The results from this study differ from those reported by Rossi et al. (2020), where the EO chemical composition of cv. Felina 32 was predominantly composed of sesquiterpene hydrocarbons (52.1%), with (*E*)-caryophyllene (34.8%) and α-humulene (11.4%) as the principal compounds. In their study, monoterpene hydrocarbons were the second most abundant chemical class (40.6%), mainly represented by α-pinene (15.1%) and myrcene (11.8%). Also in this case, cannabinoids were nearly absent (Rossi et al., 2020). A similar chemical composition for the cv. Felina 32 cultivated in the Nordic-Baltic region was reported by Barčauskaitė et al. (2022). The EO chemical composition can vary depending on factors such as harvesting period or storage conditions of the hemp biomass (Benelli et al., 2018b). For instance, Pieracci et al. (2021) reported a cv. Felina 32 chemical composition dominated by cannabinoids (53.4%) and oxygenated sesquiterpenes (30.9%) for samples harvested in 2019. By contrast, samples harvested in 2020 were dominated by oxygenated sesquiterpenes (33.2%) and sesquiterpene hydrocarbons (29.6%). The variation in the chemical composition in function of the distillation time is consistent with previous studies. For instance, Palmieri et al. (2021) reported that longer distillation times led to an enrichment of minor sesquiterpenes and predominantly cannabinoids. Similar observations were also reported by Zheljazkov et al. (2020a), who found a significant increase in the cannabinoids content for longer distillation times and suggested some conversion processes occurring after 180 min of distillation. Nevertheless, the high CBD percentages found in this study have also been reported for wild and registered hemp cultivars after HD. For example, Zheljazkov et al. (2020b) found a CBD content in wild hemp from 6.9 to 52.4%, while in the registered cultivars from 7.1 to 25.4%. Regarding cannabinoids, it is worth noting that THC was present in traces or minimal levels in all samples analyzed (0.04–0.28% in HD, 0.04–0.48% in SD, and 0.03–0.30% in MAH).

Then, a correlation analysis was performed to reduce the number of compounds (all those showing at least a statistically significant correlation) from 44 to 15, focusing on the most abundant ones (with a relative abundance greater than 1% of the total composition), such as CBD, (*E*)-caryophyllene, terpinolene, and caryophyllene oxide. CBD showed a strong negative correlation with a multitude of other compounds, including some of the most representative marker compounds in EO, such as α- and β-pinene, myrcene, and β-phellandrene. This negative correlation suggested that the increase in CBD was associated with the reduction of these compounds (Figure S4, Supplementary material).

To explore potential relationships between compound percentages and distillation conditions, a PCA analysis was performed. The first two principal components (PC1 and PC2) captured most of the data variability, with PC1, largely influenced by CBD, explaining 88% of the variability, and PC2, mainly associated with (*E*)-caryophyllene, accounting for 10%. While the PCA (Fig. 2) did not reveal distinct clusters for the two studied variables, it indicated that CBD tended to be more

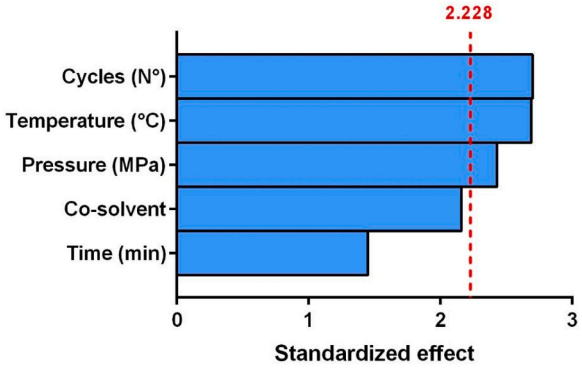

Fig. 3. Pareto plot evaluating the effect of the variables (Cycles, Temperature, Pressure, Co-solvent, and Time) on the supercritical fluid extraction (SFE) yield.

abundant at longer distillation times, particularly for SD and HD. This shift may be attributed to an increase in decarboxylative reactions within the plant matrix as distillation time progresses, converting cannabinoid acids into their neutral forms and thereby enhancing their presence in the EO.

The results of the correlation analysis implied that, with longer distillation periods, the EO contained lower amounts of α-pinene, β-pinene, myrcene, β-phellandrene and limonene. Furthermore, it seems that samples obtained after 60 min of distillation were richest in terpinolene, regardless of the type of technique used. Additionally, EO from HD showed a higher relative percentage of (*E*)-caryophyllene.

These results confirmed that shorter distillation times yielded an EO characterized mostly by monoterpene hydrocarbons while longer distillation times reduced their percentages and increased cannabinoids content. In contrast, the sesquiterpene fraction seemed to be not particularly affected by distillation time.

3.2. Byproducts processing

3.2.1. Supercritical fluid extraction (SFE) of depleted hemp biomass

3.2.1.1. Setting the SFE conditions. The recovery of cannabinoids from the depleted biomass generated during distillation was carried out using SFE with CO_2. Initially, this technique was studied to identify the experimental conditions influencing the extraction yield. Given the extensive research on the SFE of hemp biomass available in the literature, a cost-effective DoE approach, specifically an FFD, was applied to verify whether the results found from previous studies could also be valid for the SFE equipment used in this work. All tests were conducted on hemp biomass previously subjected to the SD process. The FFD results are shown in Fig. 3 using a Pareto chart. Among the variables studied, namely co-solvent, time, temperature, pressure, and cycles, only the last three showed a statistically significant effect, and in all cases, the effect was positive (an increase in the variable values resulted in an increase in SFE yield). These results only partially align with those reported in the literature, also considering that there is no clear consensus on the effect of certain parameters. While there is a general agreement on the positive impact of pressure on SFE yield (Da Porto et al., 2012; Kitryté et al., 2018; Jokić et al., 2022; Boumghar et al., 2023), as well as on the benefits of using ethanol as a co-solvent (Fernández et al., 2022), the effects of temperature (Da Porto et al., 2012; Kitryté et al., 2018; Jokić et al., 2022; Boumghar et al., 2023) and time (Kitryté et al., 2018; Boumghar et al., 2023) have produced conflicting results.

The most interesting results concerned the cycles variable, which proved to be highly influential. Since no studies in literature report its effect, further investigations were carried out. It should be emphasized that the cycles parameter from the screening included two distinct variables: the actual number of cycles and the static/dynamic ratio for each cycle. To study the effect of these two parameters separately, a two-factor CCD was used. The CCD analysis revealed that only the linear term of the static/dynamic ratio affected the extraction yield, as shown in Fig. 4 (all details of the CCD results can be found in the Supplementary material). These results indicate that a continuous flow of fresh SFE ensured the best extraction performance.

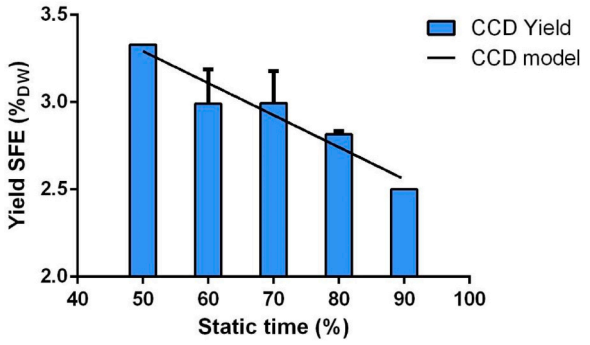

Fig. 4. Effect of the static/dynamic ratio on the supercritical fluid extraction (SFE) yield.

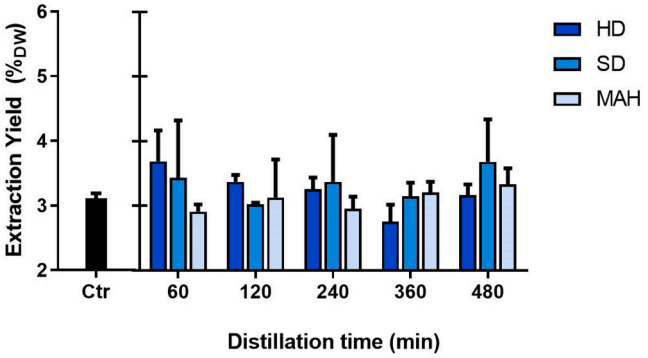

Fig. 5. Yield values (%) for the different supercritical fluid extractions (SFE).

Based on the FFD and CCD results, the optimal set of extraction conditions can be defined as follows: a temperature of 70°C, a pressure of 50 MPa, an extraction time of 50 min, and a single cycle with a static/dynamic ratio of 7 (70% of time in static mode and 30% in dynamic mode). The values for temperature and pressure were the highest used in the FFD, avoiding the instrument limit settings. The time was set to the lowest value used in the FFD since it was not statistically significant, while the static/dynamic ratio was set to an intermediate value based on the data in Fig. 4 and considering the need to reduce CO_2 consumption. For instance, a lower ratio, such as 5, would have improved yield by only 0.2 %, but consumed almost twice the amount of CO_2.

3.2.1.2. Analysis of SFE extracts. Following the EO distillation, the depleted hemp biomass was subjected to SFE under the conditions defined in Section 3.2.1. The obtained extracts were analyzed both quantitatively and qualitatively for six marker cannabinoids to identify any potential effects of the type of distillation performed. Additionally, the results were compared with those obtained from hemp untreated biomass.

The yield values for the different SFEs are shown in Fig. 5. A two-way ANOVA revealed no statistically significant influence of the type or time of distillation. In all cases, the SFE yield ranged from 2.8% to 3.7%$_{DW}$. These values were comparable to the yield obtained from SFE of untreated hemp (3.11%$_{DW}$, Ctr in Fig. 5). Thus, for hemp, the yield in SFE appeared to be primarily determined by the selected operative parameters.

Overall, the yields reported in this study were lower than those

Table 3
Cannabinoids content in the supercritical fluid extraction (SFE) extracts from hemp depleted biomass determined by HPLC-DAD analysis.

Cannabinoids content in the extracts (g/100 g extract ± SD)[a]								
Distillation[b]	Time (min)	CBDV[b]	CBD[c]	CBG[d]	CBDA[e]	CBC[f]	THC[g]	Total cannabinoids
HD	60	0.39 ± 0.08	16.06 ± 0.38	0.47 ± 0.16	0.50 ± 0.19	1.08 ± 0.11	0.19 ± 0.01	18.66 ± 0.23
HD	120	0.34 ± 0.03	16.08 ± 0.50	0.41 ± 0.09	0.55 ± 0.43	1.05 ± 0.03	0.22 ± 0.09	18.63 ± 0.88
HD	240	0.40 ± 0.10	18.55 ± 1.99	0.44 ± 0.02	0.24 ± 0.09	1.18 ± 0.08	0.33 ± 0.01	21.12 ± 2.07
HD	360	0.35 ± 0.06	17.77 ± 2.18	0.36 ± 0.03	0.05 ± 0.08	1.14 ± 0.11	0.19 ± 0.03	19.86 ± 2.33
HD	480	0.35 ± 0.03	17.47 ± 0.54	0.37 ± 0.02	0.04 ± 0.05	1.17 ± 0.03	0.22 ± 0.10	19.62 ± 0.64
SD	60	0.36 ± 0.07	18.06 ± 3.15	0.42 ± 0.05	0.22 ± 0.02	1.10 ± 0.16	0.36 ± 0.03	20.51 ± 3.43
SD	120	0.37 ± 0.03	17.19 ± 0.83	0.43 ± 0.05	0.20 ± 0.04	1.06 ± 0.06	0.32 ± 0.00	19.58 ± 0.86
SD	240	0.38 ± 0.07	17.27 ± 0.68	0.37 ± 0.01	0.06 ± 0.08	1.12 ± 0.00	0.24 ± 0.06	19.44 ± 0.64
SD	360	0.39 ± 0.04	18.48 ± 1.03	0.40 ± 0.07	0.06 ± 0.08	1.16 ± 0.01	0.31 ± 0.03	20.79 ± 1.19
SD	480	0.43 ± 0.10	17.57 ± 0.64	0.42 ± 0.10	0.00 ± 0.00	1.22 ± 0.14	0.34 ± 0.15	19.98 ± 0.15
MAH	60	0.39 ± 0.05	16.74 ± 2.46	0.35 ± 0.02	0.24 ± 0.08	1.04 ± 0.10	0.35 ± 0.05	19.11 ± 2.77
MAH	120	0.35 ± 0.00	15.82 ± 1.62	0.41 ± 0.02	0.10 ± 0.02	0.98 ± 0.08	0.32 ± 0.05	17.97 ± 1.66
MAH	240	0.43 ± 0.03	19.24 ± 1.22	0.48 ± 0.10	0.09 ± 0.01	1.19 ± 0.05	0.31 ± 0.06	21.75 ± 1.26
MAH	360	0.35 ± 0.05	16.16 ± 1.87	0.43 ± 0.02	0.07 ± 0.10	1.04 ± 0.13	0.34 ± 0.01	18.40 ± 2.13
MAH	480	0.39 ± 0.05	15.87 ± 0.40	0.47 ± 0.18	0.00 ± 0.00	1.02 ± 0.04	0.39 ± 0.03	18.13 ± 0.11
Untreated biomass (not distilled)		0.30 ± 0.03	13.43 ± 0.71	0.32 ± 0.01	1.88 ± 0.43	0.90 ± 0.02	0.34 ± 0.04	17.15 ± 0.30

[a] Cannabinoids content in the extracts obtained by HPLC-DAD analysis ± SD, standard deviation;
[b] CBDV, cannabidivarin;
[c] CBD, cannabidiol;
[d] CBG, cannabigerol;
[e] CBDA, cannabidiolic acid;
[f] CBC, cannabichromene;
[g] THC, tetraidrocannabinol.

reported in previous studies for SFE. For instance, Kitrytè and collaborators (2018) applied experimental conditions of SFE extraction similar to those proposed in our work (46.5 MPa, 70 °C, 120 min), obtaining a yield for the cv. Beniko of 8.3 $\%_{DW}$. Moreover, the SFE yields reported by Vàgi and collaborators (2020) on residues of two varieties, Felina 32 and Kompolti, were also higher (6.59 $\%_{DW}$). The differences detected in SFE may depend on the variety of hemp, the pre-treatment of the matrix and on the operating conditions of the supercritical extractor.

All the SFE extracts from depleted and not distilled hemp biomass were characterized in terms of marker cannabinoids, including CBDV, CBD, CBG, CBDA, CBC, and THC. Concentrations (g/100 g of SFE extract) were determined by HPLC-DAD analysis. As reported in Table 3, the total cannabinoids content ranged from 17.15 to 21.75 g/100 g of SFE extract with CBD as the most abundant compound, ranging from 13.43 to 19.24 g/100 g of SFE extract. CBDV, CBD, CBG, CBDA, and CBC were found in minor amounts as well as THC, whose levels were always lower than 0.39 g/100 g of SFE extract.

The CBD content seemed to not change significantly as a function of distillation technique and time, likely due to the partial recovery of CBD in the EOs. Thus, its content did not increase significantly in the depleted biomass obtained after longer distillation times. The amount of CBD found in the SFE extracts (17.15–21.75 g/100 g of SFE extract) was higher than those reported by Jokić et al. (2022). The latter employed cv. Futura 85 and found a content of CBD of 6.58 g/100 g of SFE extract under optimized conditions. Similarly, Qamar et al. (2022) optimized the SFE of cannabinoids yielding 0.78 g/100 g of SFE extract. In both studies high levels of CBDA were observed, however, in this study, CBDA concentrations were significantly reduced by the pretreatment in favor of the CBD content. The high concentration of CBD found in this study could be due to the pretreatment applied as well as the use of different hemp cultivars. It is noteworthy that the level of CBD found in the SFE extracts was significantly higher than that in the untreated biomass due to decarboxylation occurring during distillation. As a matter of fact, the level of CBDA in untreated biomass was the highest (1.88 g/100 g). Interestingly, the concentration of CBDA progressively diminished in the depleted biomass for times exceeding 120 min, and disappeared in samples distilled for 480 min (Table 3). This proves its complete decarboxylation after that time.

The above-mentioned results demonstrate that all distillation techniques preserved the cannabinoid content within the hemp biomass and increased the CBD concentration compared with CBDA. Notably, the concentration of CBD in SFE extracts from distilled material was 1.2–1.4 times higher than those from untreated (non-distilled) biomass. This result has previously been observed by Zheljazkov and Maggi (2021) who found that the content of CBD in the distilled biomass was 3.4–9 times higher than that of the untreated material. In fact, the same authors used scanning electron microscopy (SEM) analysis of hemp inflorescences showing that most of the glandular trichomes in distilled biomass were not damaged. Thus, this study proved the high impact of the preventive distillation on the decarboxylation process from CBDA to

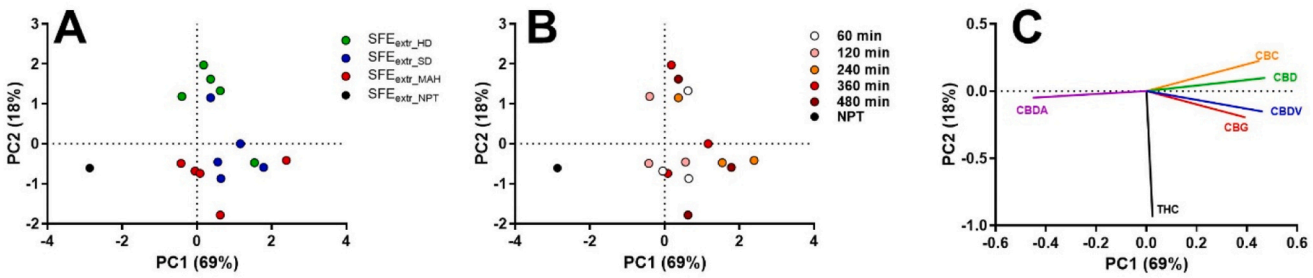

Fig. 6. PCA analysis performed on the supercritical fluid extraction extracts (SFE_{extr}) obtained from the hemp biomass deriving from different techniques (A) (HD, hydrodistillation; SD, steam distillation, and MAH, microwave-assisted hydrodistillation) and distillation times (B) (60, 120, 240, 360, and 480 min) or untreated (NPT).

Table 4
Average content of flavoniods in the dry extracts (DE) from residual water after distillation and determined by HPLC-MS analysis.

	Content ($mg/g_{DE} \pm SD$)[a]														
	HD[b]					SD[b]					MAH[b]				
Flavonoids[c]	**60**[d]	**120**[d]	**240**[d]	**360**[d]	**480**[d]	**60**	**120**	**240**	**360**	**480**	**60**	**120**	**240**	**360**	**480**
caffeoyl-*O*-hexoside	0.40 ± 0.05	0.20 ± 0.05	0.20 ± 0.05	0.47 ± 0.15	0.30 ± 0.07	0.41 ± 0.06	0.26 ± 0.08	0.34 ± 0.12	0.40 ± 0.11	0.59 ± 0.06	0.40 ± 0.08	0.50 ± 0.21	0.19 ± 0.10	0.32 ± 0.08	0.37 ± 0.04
protocatecuic acid hexoside	0.28 ± 0.22	0.25 ± 0.01	0.25 ± 0.01	0.29 ± 0.02	0.25 ± 0.01	0.33 ± 0.07	0.24 ± 0.04	0.30 ± 0.07	0.35 ± 0.00	0.27 ± 0.05	0.34 ± 0.03	0.25 ± 0.03	0.24 ± 0.02	0.31 ± 0.02	0.28 ± 0.04
5-hydroxyhexanoic acid hexoside	0.41 ± 0.04	0.11 ± 0.16	0.25 ± 0.02	0.32 ± 0.02	0.16 ± 0.22	0.38 ± 0.01	0.34 ± 0.02	0.37 ± 0.01	0.37 ± 0.01	0.37 ± 0.01	0.39 ± 0.02	0.40 ± 0.04	0.35 ± 0.04	0.20 ± 0.24	0.36 ± 0.04
5,7,4′-trihydroxyflavanone 6.8-di-*C*-glucoside	0.04 ± 0.03	0.01 ± 0.01	0.01 ± 0.00	0.03 ± 0.01	0.01 ± 0.00	0.01 ± 0.00	0.01 ± 0.00	0.07 ± 0.04	0.09 ± 0.04	0.10 ± 0.01	0.12 ± 0.00	0.09 ± 0.02	0.08 ± 0.01	0.02 ± 0.02	0.02 ± 0.01
2-hydroxy isocaproic acid hexoside	0.17 ± 0.03	0.04 ± 0.06	0.10 ± 0.00	0.10 ± 0.01	0.05 ± 0.07	0.13 ± 0.02	0.12 ± 0.00	0.12 ± 0.01	0.12 ± 0.01	0.12 ± 0.00	0.14 ± 0.02	0.14 ± 0.01	0.12 ± 0.00	0.13 ± 0.01	0.12 ± 0.01
hydroxy jasmonic acid hexoside	1.14 ± 0.42	0.76 ± 0.04	0.83 ± 0.28	1.33 ± 0.05	0.97 ± 0.42	1.62 ± 0.55	1.73 ± 0.79	1.25 ± 0.47	1.45 ± 0.19	1.30 ± 0.20	2.02 ± 0.75	1.45 ± 0.43	1.45 ± 0.66	2.08 ± 0.08	0.90 ± 1.06
apigenin 6,8-di-*C*-glucoside	0.06 ± 0.03	0.30 ± 0.26	0.32 ± 0.19	0.36 ± 0.02	0.34 ± 0.01	0.35 ± 0.04	0.24 ± 0.05	0.51 ± 0.23	0.38 ± 0.02	0.80 ± 0.18	0.62 ± 0.23	0.33 ± 0.10	0.29 ± 0.12	0.17 ± 0.06	0.10 ± 0.02
luteolin *C*-hexoside *O*-rhamnoside	0.65 ± 0.47	0.74 ± 0.19	0.61 ± 0.17	1.53 ± 0.11	1.34 ± 0.33	1.27 ± 0.08	1.00 ± 0.47	1.34 ± 0.14	1.33 ± 0.20	0.78 ± 0.11	0.97 ± 0.14	0.66 ± 0.38	0.59 ± 0.19	0.13 ± 0.03	0.16 ± 0.01
roseoside	0.57 ± 0.16	0.13 ± 0.08	0.48 ± 0.18	0.17 ± 0.12	0.30 ± 0.23	0.77 ± 0.78	0.15 ± 0.15	0.80 ± 0.60	0.04 ± 0.06	0.64 ± 0.62	0.60 ± 0.13	0.86 ± 0.65	0.66 ± 0.69	0.32 ± 0.01	0.86 ± 0.34
luteolin−6,8-di-*C*-hexoside	1.27 ± 0.61	1.45 ± 0.56	1.44 ± 0.96	1.74 ± 1.30	1.59 ± 1.05	1.37 ± 0.14	1.43 ± 0.23	2.15 ± 0.17	1.95 ± 0.00	2.00 ± 0.04	1.63 ± 0.44	1.76 ± 1.56	1.23 ± 0.04	0.63 ± 0.69	0.65 ± 0.27
luteolin-*C*-hexoside-*O*-rhamnoside	2.77 ± 0.17	2.14 ± 0.30	2.13 ± 0.44	3.23 ± 0.80	2.80 ± 0.49	3.64 ± 1.28	2.50 ± 0.01	3.39 ± 0.72	4.24 ± 0.12	3.71 ± 0.47	4.42 ± 1.01	3.32 ± 2.02	2.37 ± 1.11	1.22 ± 0.08	1.02 ± 0.60
isoorientin/orientin (luteolin-*C*-hexoside)	0.46 ± 0.58	0.63 ± 0.69	0.63 ± 0.27	0.96 ± 0.68	0.71 ± 0.26	0.50 ± 0.62	0.62 ± 0.39	0.81 ± 0.54	0.85 ± 0.05	0.99 ± 0.18	0.22 ± 0.28	0.37 ± 0.27	0.68 ± 0.11	0.27 ± 0.26	0.22 ± 0.13
vitexin−2′′-glucoside	0.46 ± 0.30	0.91 ± 0.68	1.34 ± 0.14	1.05 ± 0.29	1.64 ± 0.35	0.78 ± 0.45	0.67 ± 0.23	0.65 ± 0.38	0.80 ± 0.08	0.60 ± 0.27	0.01 ± 0.01	0.19 ± 0.15	0.36 ± 0.19	0.33 ± 0.45	0.01 ± 0.01
apigenin-*C*-(hexoside-*O*-rhamnoside)	3.00 ± 0.90	2.33 ± 0.11	3.18 ± 0.21	4.42 ± 0.87	3.34 ± 0.08	3.06 ± 0.84	2.96 ± 0.32	4.46 ± 0.65	3.92 ± 0.09	4.35 ± 0.53	3.11 ± 0.32	2.22 ± 0.37	2.82 ± 0.20	1.71 ± 0.08	1.40 ± 0.45
vitexin	0.08 ± 0.00	0.26 ± 0.27	0.15 ± 0.10	0.30 ± 0.38	0.18 ± 0.13	0.23 ± 0.32	0.41 ± 0.05	0.30 ± 0.11	0.27 ± 0.07	0.21 ± 0.02	0.12 ± 0.05	0.12 ± 0.03	0.08 ± 0.08	0.00 ± 0.00	0.04 ± 0.01
dihydrokeamferol 3-*O*-hexoside	0.50 ± 0.39	0.29 ± 0.01	0.20 ± 0.11	0.36 ± 0.22	0.28 ± 0.06	0.47 ± 0.19	0.37 ± 0.42	0.53 ± 0.21	0.74 ± 0.09	0.63 ± 0.17	0.57 ± 0.01	0.64 ± 0.48	0.53 ± 0.32	0.49 ± 0.27	0.59 ± 0.22
luteolin−4′-*O*-hexoside	0.02 ± 0.03	0.19 ± 0.04	0.00 ± 0.00	0.11 ± 0.16	0.00 ± 0.01	0.07 ± 0.09	0.19 ± 0.27	0.23 ± 0.23	0.08 ± 0.08	0.21 ± 0.11	0.06 ± 0.01	0.05 ± 0.06	0.00 ± 0.01	0.01 ± 0.01	0.85 ± 1.20
luteolin-*O*-glucuronide	0.72 ± 0.11	0.59 ± 0.13	0.88 ± 0.08	0.85 ± 0.01	0.85 ± 0.10	0.59 ± 0.09	0.74 ± 0.17	0.68 ± 0.12	0.68 ± 0.07	0.65 ± 0.16	0.71 ± 0.06	0.72 ± 0.15	0.67 ± 0.04	0.65 ± 0.07	0.88 ± 0.34
3′-*O*-methyl luteolin-*O*-glucuronide	0.16 ± 0.10	0.33 ± 0.15	0.45 ± 0.06	0.34 ± 0.24	0.55 ± 0.07	0.40 ± 0.02	0.45 ± 0.07	0.44 ± 0.16	0.46 ± 0.03	0.34 ± 0.27	0.34 ± 0.07	0.28 ± 0.26	0.37 ± 0.08	0.28 ± 0.14	0.31 ± 0.00
cannabisin D derivative	0.07 ± 0.02	0.14 ± 0.09	0.21 ± 0.10	0.10 ± 0.01	0.09 ± 0.04	0.23 ± 0.02	0.17 ± 0.11	0.12 ± 0.12	0.08 ± 0.04	0.08 ± 0.05	0.10 ± 0.08	0.23 ± 0.06	0.19 ± 0.19	0.06 ± 0.01	0.16 ± 0.03
sinapic acid hexoside	0.70 ± 0.52	0.36 ± 0.23	0.42 ± 0.33	0.72 ± 0.18	0.74 ± 0.12	0.33 ± 0.27	0.40 ± 0.41	0.76 ± 0.60	0.92 ± 0.43	0.71 ± 0.09	0.45 ± 0.18	0.37 ± 0.07	0.69 ± 0.18	0.19 ± 0.06	0.15 ± 0.08
cannabisin B	0.15 ± 0.16	0.28 ± 0.19	0.55 ± 0.16	1.00 ± 0.73	2.65 ± 1.70	0.03 ± 0.00	0.22 ± 0.03	0.37 ± 0.06	0.73 ± 0.06	0.39 ± 0.01	0.03 ± 0.01	0.08 ± 0.07	0.14 ± 0.06	0.13 ± 0.04	0.25 ± 0.13
5,7-dihydroxy 8-methoxyflavone 7-glucuronide	0.13 ± 0.15	0.09 ± 0.09	0.11 ± 0.00	0.13 ± 0.01	0.12 ± 0.04	0.04 ± 0.00	0.03 ± 0.01	0.05 ± 0.03	0.03 ± 0.00	0.03 ± 0.01	0.04 ± 0.00	0.09 ± 0.08	0.03 ± 0.00	0.05 ± 0.03	0.05 ± 0.01
cannflavin B	0.02 ± 0.00	0.02 ± 0.00	0.02 ± 0.00	0.01 ± 0.00	0.02 ± 0.00	0.03 ± 0.02	0.03 ± 0.00	0.02 ± 0.00	0.02 ± 0.00	0.01 ± 0.00	0.02 ± 0.00	0.02 ± 0.00	0.01 ± 0.00	0.02 ± 0.00	0.02 ± 0.00
cannflavin A	0.01 ± 0.01	0.00 ± 0.00	0.01 ± 0.00	0.01 ± 0.01	0.01 ± 0.00	0.00 ± 0.00	0.01 ± 0.00	0.01 ± 0.01	0.00 ± 0.01	0.01 ± 0.00	0.00 ± 0.00	0.00 ± 0.00	0.00 ± 0.00	0.03 ± 0.01	0.08 ± 0.04

(*continued on next page*)

Table 4 (*continued*)

	Content (mg/g_{DE} ± SD)[a]												
	HD[b]				**SD**[b]				**MAH**[b]				
total	14.24 ± 1.29	12.55 ± 2.26	14.76 ± 1.65	19.95 ± 4.56	19.30 ± 0.21	17.04 ± 0.73	15.28 ± 0.84	20.10 ± 2.27	20.32 ± 0.04	19.91 ± 1.43	17.45 ± 0.59	15.14 ± 4.52	14.13 ± 2.15	9.76 ± 0.79	9.84 ± 0.81
C-flavonoids	8.78 ± 0.29	8.77 ± 1.71	9.81 ± 0.97	13.61 ± 4.43	11.95 ± 1.59	11.20 ± 1.46	9.85 ± 0.66	13.70 ± 2.05	13.85 ± 0.50	13.55 ± 0.65	11.22 ± 1.82	9.06 ± 4.60	8.49 ± 1.57	4.48 ± 0.62	3.60 ± 0.58
O-flavonoids	1.54 ± 0.52	1.49 ± 0.33	1.64 ± 0.25	1.80 ± 0.60	1.81 ± 0.12	1.57 ± 0.16	1.78 ± 0.39	1.93 ± 0.14	1.99 ± 0.02	1.86 ± 0.35	1.73 ± 0.10	1.78 ± 0.09	1.60 ± 0.20	1.49 ± 0.15	2.68 ± 1.32
cannflavins	0.03 ± 0.02	0.02 ± 0.00	0.02 ± 0.00	0.02 ± 0.01	0.03 ± 0.00	0.04 ± 0.01	0.04 ± 0.01	0.03 ± 0.01	0.02 ± 0.01	0.02 ± 0.00	0.02 ± 0.01	0.02 ± 0.00	0.02 ± 0.00	0.05 ± 0.01	0.10 ± 0.04
others	3.89 ± 1.04	2.27 ± 0.21	3.28 ± 0.43	4.51 ± 0.49	5.50 ± 1.91	4.23 ± 0.55	3.61 ± 1.12	4.43 ± 0.62	4.46 ± 0.53	4.48 ± 0.43	4.48 ± 1.12	4.28 ± 0.01	4.03 ± 0.38	3.75 ± 0.31	3.46 ± 1.51
	HD				**SD**						**MAH**				
C-flavonoids	10.59 ± 1.58				12.43 ± 0.67					*C*-flavonoids	7.37 ± 1.64				
O-flavonoids	1.66 ± 0.20				1.83 ± 0.15					*O*-flavonoids	1.85 ± 0.53				
cannflavins	0.03 ± 0.01				0.03 ± 0.00					cannflavins	0.04 ± 0.02				
others	3.89 ± 0.68				4.24 ± 0.27					others	4.00 ± 0.62				

[a] Average content (expressed ad mg/g of dry extract (DE)) is mean od two independent analyses and standard deviation (SD).

[b] HD, hydrodistillation; SD, steam distillation; MAH, microwave-assisted hydrodistillation.

[c] Compounds are ordered according to their retention time.

[d] Distillation times: 60, 120, 240, 360, and 480 min.

CBD. This shows that distillation of hemp biomass leads to the extraction of terpenes leaving cannabinoids in the residual biomass already converted to their neutral forms. This phenomenon has previously been demonstrated by Zheljazkov et al., (2022). Indeed, their study demonstrated that SD preserves the content of cannabinoids in the plant matrix also favoring their decarboxylation.

HPLC data were elaborated using PCA. The results (Fig. 6) clearly showed distinct clusters based on the pretreatment (Fig. 6A). Specifically, SFE extract from the untreated biomass was positioned at lower PC1 values, being richer in CBDA and poorer in other cannabinoids than the distilled samples. All SFE extracts from the depleted biomass showed comparable amounts of CBDV, CBD, CBG, CBDA, and CBC, and could only be differentiated based on the THC content. Notably, biomass from MAH and SD contained higher amounts of THC compared with those subjected to HD. No clustering was observed based on distillation time (Fig. 6B).

3.2.2. *Chemical analysis of residual water*

In the framework of a zero-waste approach of hemp biomass processing, finding applications for generated residual wastes is an added value. Thus, in this study, we analyzed DEs derived from residual water of the distillation process. The predominant compounds identified in the DEs were *C*-glycosylated (10.59, 12.43, and 7.37 mg/g of DE from HD, SD, and MAH, respectively) and *O*-glycosylated (1.66, 1.83, and 1.85 mg/g of DE from HD, SD, and MAH, respectively) flavonoids, and cannflavins (0.03, 0.03, and 0.04 mg/g of DE from HD, SD, and MAH, respectively) (Mazzara et al., 2022a) (Table 4). Regarding *C*-glycosylated flavonoids, which were the most abundant compounds detected, luteolin-*C*-(hexoside-*O*-rhamnoside) and apigenin-*C*-(hexoside-*O*-rhamnoside) were the predominant derivatives with a concentration between 1 and 5 mg/g. Other minor flavonoids were also detected, i.e., phenolic hydroxycinnamic derivatives (caffeoyl hexoside and roseroside) (Stanoeva et al., 2017) as well as cannabisin B and a derivative of cannabisin D (Benkirane et al., 2022). Among minor compounds, 5-hydroxyhexanoic acid hexoside and 2-hydroxyisocaproic acid hexoside were also identified considering their fragmentation pattern with molecular ion $[M\text{-}H]^-$ at 293 *m/z* and fragments at 131 and 85 *m/z* (Emad et al., 2022). Hydroxyjasmonic acid hexoside was identified by analyzing its fragmentation patterns for the ion $[M\text{-}H]^-$ observed at *m/z* 387 and the fragments at *m/z* 369, 225, 207, and 163 (Stanoeva et al., 2017).

Among the different distillation techniques, SD and HD proved to be the most efficient for extracting *C*-glycosylated flavonoids, followed by MAH, with mean concentrations of 12.43, 10.59, and 7.37 mg/g, respectively. The lower content of *C*-glycosylated flavonoids in the DEs deriving from the MAH could be attributed to different factors. Among them, the higher amount of water employed in HD and SD could led to stronger hydrolysis than in the MAH. On the other hand, the content of *O*-glycosylated flavonoids, cannflavins, and other phytochemicals was not affected by the choice of the distillation technique.

The same statistical approach for the EOs was applied to the residual water composition by performing a correlation analysis and removing all the correlated compounds. In this case, only two compounds, i.e. 2-hydroxyisocaproic acid hexoside and 5-hydroxyhexanoic acid hexoside, were correlated with each other. The latter was retained due to its higher concentration and inserted into the PCA analysis with the other non-correlated compounds. The PCA analysis identified three distinct clusters related to the distillation technique (Fig. 7A). Specifically, the DEs obtained from HD and SD showed comparable values in PC1, indicating medium to high concentrations of apigenin-*C*-(hexoside-*O*-rhamnoside), luteolin-6,8-di-*C*-hexoside, luteolin-*C*-(hexoside-*O*-rhamnoside), and low concentrations of luteolin-4-*O*-hexoside. However, the DEs from the two techniques differed for PC2. Specifically, HD DEs were richer in luteolin-*C*-(hexoside-*O*-rhamnoside) and hydroxyjasmonic acid hexoside, whereas SD DEs showed higher concentrations of cannabisin B, vitexin-2-glucoside, and isoorientin/orientin (luteolin-*C*-hexoside).

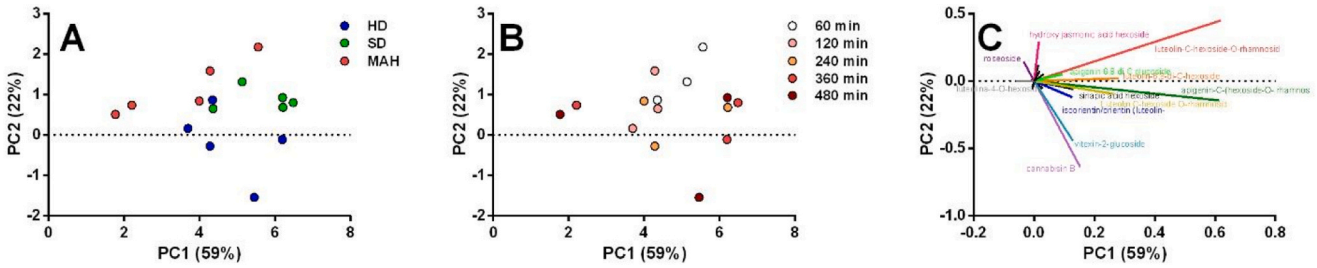

Fig. 7. PCA analysis performed on the dry extracts (DEs) obtained from the residual water deriving from different distillation techniques (A) (HD, hydrodistillation; SD, steam-distillation, and MAH, microwave-assisted hydrodistillation) and distillation times (B) (60, 120, 240, 360, and 480 min).

The samples from MAH, although separated from the others in the score plot of Fig. 7A, followed a specific trend, moving from samples with low values of PC1 and median values of PC2 to those positioned at high values of PC1 and PC2. This trend can be explained by considering the data labelled in terms of distillation time (Fig. 7B). At shorter distillation times, the MAH DEs resembled those from HD, characterized by high values in PC1 and PC2. At longer distillation times, the DEs were completely different, being marked by higher concentrations of luteolin-4-*O*-hexoside and low or average concentrations of all the other components. This could be caused by the extended exposure time to microwaves that could lead to a progressive loss of other flanovoids.

The composition in phenolics, especially flavonoids, of DEs deriving from the distillation of different hemp varieties has been previously reported (Mazzara et al., 2022a, 2022b), demonstrating the potential further exploitation of the residual water. The qualitative composition of the DEs of our study align with that reported in the work of Mazzara et al. (2022b), who demonstrated that the DE derived from the MAH of the cv. Futura 75 was also rich of luteolin-*C*-(hexoside-*O*-rhamnoside) and apigenin-*C*-(hexoside-*O*-rhamnoside). However, the levels of the two flavonoids do not perfecly align with those found in our study, and this could depend on the different hemp variety employed. It is worthy to note that the phenolic composition of the DE and of the residual biomass can completely differ. This has been demonstrated by Mazzara et al. (2022a), who proved that the DEs contained a higher amount of glycosidic flavonoids, such as luteolin glycosides or rutin, which are in general more soluble in water at high temperatures. The latter were less present in the residual biomass, which resulted rich of cannflavins, specifically cannflavin A and B. However, it is worthy to note that the differences in flavonoids content could be influenced by the different hemp varieties employed for the studies, as well as by the different treatment applied to the biomass.

Flavonoid *C*-glycosides, as luteolin and apigenin derivatives, have been reported for many therapeutic properties, i.e., antioxidant, wound healing, and anti-inflammatory activities, thus, favoring the potential employment of the residual water for different applications (Tahir et al., 2012; Zain et al., 2020). For instance, Cásedas et al. (2022) tested the DE and the *n*-hexane extract obtained from the residual water and the spent biomass of industrial hemp distillation, respectively, for their antioxidant profile and their neuroprotective potential on pharmacological targets in the central nervous system (CNS). This study proved the higher efficacy of the DE for the acetylcholinesterase (AChE) and monoamine oxidase A (MAO-A) inhibitory activity as well as no cytotoxicity on neuro-2a cell line. The latter was also accompanied by cytoprotective properties against hydrogen peroxide and antioxidant response decreasing reactive oxygen species (ROS) production. Further studies are needed to asses the potential applications of this valuable by-product of hemp distillation.

4. Conclusions

The main aim of this study was to address the gap in the literature on the circular economy framework of hemp EO production. Specifically, the effect of different distillation techniques and durations was assessed on the cannabinoid content of the depleted biomass and on the phenolic composition of the residual water.

The results demonstrated that all techniques and durations effectively induced the decarboxylation of cannabinoid acids leading to the formation of their active counterparts. Indeed, the SFEs obtained from the depleted biomass were rich in neutral cannabinoids. Moreover, the residual water was enriched in luteolin and apigenin derivatives, bioactive compounds with well-documented beneficial properties that could be employed in many fields of application. Regarding the EO compositions, the three distillation techniques, operating at different times, led to distinct volatile profiles which could be exploited for different applications depending on the major classes of components.

The findings of this study can be extended to other registered hemp varieties and medical cannabis, enabling the exploitation of distillation byproducts in multiple industrial sectors.

CRediT authorship contribution statement

Cespi Marco: Writing – review & editing, Writing – original draft, Visualization, Validation, Software, Methodology, Formal analysis, Data curation. **Sut Stefania:** Writing – original draft, Visualization, Formal analysis, Data curation. **Maggi Filippo:** Writing – review & editing, Writing – original draft, Visualization, Supervision, Resources, Project administration, Investigation, Conceptualization. **Petrelli Riccardo:** Writing – review & editing, Visualization, Supervision. **Boldrini Luca:** Methodology, Formal analysis, Data curation. **Spinozzi Eleonora:** Writing – review & editing, Writing – original draft, Visualization, Validation, Methodology, Investigation, Formal analysis, Data curation. **Betti Erica:** Writing – original draft, Methodology. **Ferrati Marta:** Writing – review & editing, Writing – original draft, Visualization, Data curation. **Zheljazkov Valtcho D.:** Writing – review & editing, Writing – original draft, Visualization, Conceptualization. **Ricciutelli Massimo:** Writing – review & editing, Formal analysis. **Dall'Acqua Stefano:** Writing – review & editing, Writing – original draft, Formal analysis, Data curation.

Declaration of Competing Interest

The authors declare that they have no known competing financial interests or personal relationships that could have appeared to influence the work reported in this paper.

Acknowledgements

Authors wish to thank Alessandro Primavera for his help during distillation, the farm La Biologica Società Cooperativa Agricola for providing hemp inflorescences of cv. Felina 32, and Milestone S.r.l. (Sorisole, Italy) for support in the use of the microwave ETHOS X.

Appendix A. Supporting information

Supplementary data associated with this article can be found in the online version at doi:10.1016/j.indcrop.2025.121094.

Data availability

Data will be made available on request.

References

Barbalace, M.C., Freschi, M., Rinaldi, I., Mazzara, E., Maraldi, T., Malaguti, M., Prata, C., Maggi, F., Petrelli, R., Hrelia, S., Angeloni, C., 2023. Identification of anti-neuroinflammatory bioactive compounds in essential oils and aqueous distillation residues obtained from commercial varieties of *Cannabis sativa* L. Int. J. Mol. Sci. 24, 16601. https://doi.org/10.3390/ijms242316601.

Barčauskaitė, K., Bakšinskaitė, A., Szumny, A., Tilvikienė, V., 2022. Variation of secondary metabolites in *Cannabis sativa* L. inflorescences under applied agrotechnological measures. Ind. Crops Prod. 188, 115570. https://doi.org/10.1016/j.indcrop.2022.115570.

Benelli, G., Pavela, R., Lupidi, G., Nabissi, M., Petrelli, R., Ngahang Kamte, S.L., Cappellacci, L., Fiorini, D., Sut, S., Dall'Acqua, M., Maggi, F., 2018b. The crop-residue of fiber hemp cv. Futura 75: from a waste product to a source of botanical insecticides. Environ. Sci. Pollut. Res. 25, 10515–10525. https://doi.org/10.1007/s11356-017-0635-5.

Benelli, G., Pavela, R., Petrelli, R., Cappellacci, L., Santini, G., Fiorini, D., Sut, S., Dall'Acqua, S., Canale, A., Maggi, F., 2018a. The essential oil from industrial hemp (*Cannabis sativa* L.) by-products as an effective tool for insect pest management in organic crops. Ind. Crops Prod. 122, 308–315. https://doi.org/10.1016/j.indcrop.2018.05.032.

Benkirane, C., Moumen, A.B., Fauconnier, M.L., Belhaj, K., Abid, M., Caid, H.S., Elamrani, A., Mansouri, F., 2022. Bioactive compounds from hemp (*Cannabis sativa* L.) seeds: optimization of phenolic antioxidant extraction using simplex lattice mixture design and HPLC-DAD/ESI-MS^2 analysis. RSC Adv. 12, 25764–25777. https://doi.org/10.1039/D2RA04081F.

Bertoli, A., Tozzi, S., Pistelli, L., Angelini, L.G., 2010. Fibre hemp inflorescences: from crop-residues to essential oil production. Ind. Crops Prod. 32, 329–337. https://doi.org/10.1016/j.indcrop.2010.05.012.

Boumghar, H., Sarrazin, M., Banquy, X., Boffito, D.C., Patience, G.S., Boumghar, Y., 2023. Optimization of supercritical carbon dioxide fluid extraction of medicinal cannabis from Quebec. Processes 11, 1953. https://doi.org/10.3390/pr11071953.

Cásedas, G., Moliner, C., Maggi, F., Mazzara, E., López, V., 2022. Evaluation of two different *Cannabis sativa* L. extracts as antioxidant and neuroprotective agents. Front. Pharmacol. 13, 1009868.

Chen, C., Pan, Z., 2021. Cannabidiol and terpenes from hemp–ingredients for future foods and processing technologies. J. Future Foods 1, 113–127. https://doi.org/10.1016/j.jfutfo.2022.01.001.

Da Porto, C., Voinovich, D., Decorti, D., Natolino, A., 2012. Response surface optimization of hemp seed (*Cannabis sativa* L.) oil yield and oxidation stability by supercritical carbon dioxide extraction. J. Supercrit. Fluids 68, 45–51. https://doi.org/10.1016/j.supflu.2012.04.008.

Draper, N.R., Pukelsheim, F., 1990. Another look at rotatability. Technometrics 32, 195–202. https://doi.org/10.1080/00401706.1990.10484635.

Dudziec, P., Warmiński, K., Stolarski, M.J., 2024. Industrial hemp as a multi-purpose crop: last achievements and research in 2018−2023. J. Nat. Fibers 21, 2369186. https://doi.org/10.1080/15440478.2024.2369186.

Emad, A.M., Rasheed, D.M., El-Kased, R.F., El-Kersh, D.M., 2022. Antioxidant, antimicrobial activities and characterization of Polyphenol-enriched extract of Egyptian celery (*Apium graveolens* L., Apiaceae) aerial parts via UPLC/ESI/TOF-MS. Molecules 27, 698. https://doi.org/10.3390/molecules27030698.

Erridge, S., Mangal, N., Salazar, O., Pacchetti, B., Sodergren, M.H., 2020. Cannflavins–from plant to patient: a scoping review. Fitoterapia 146, 104712. https://doi.org/10.1016/j.fitote.2020.104712.

Fernández, S., Carreras, T., Castro, R., Perelmuter, K., Giorgi, V., Vila, A., Rosales, A., Pazos, M., Moyna, G., Carrera, I., Bollati-Fagolin, M., Garcia-Carnelli, C., Carrera, I., Vieitez, I., 2022. A comparative study of supercritical fluid and ethanol extracts of cannabis inflorescences: chemical profile and biological activity. J. Supercrit. Fluids,179, 105385. https://doi.org/10.1016/j.supflu.2021.105385.

Filly, A., Fernandez, X., Minuti, M., Visinoni, F., Cravotto, G., Chemat, F., 2014. Solvent-free microwave extraction of essential oil from aromatic herbs: from laboratory to pilot and industrial scale. Food Chem. 150, 193–198. https://doi.org/10.1016/j.foodchem.2013.10.139.

Fiorini, D., Molle, A., Nabissi, M., Santini, G., Benelli, G., Maggi, F., 2019. Valorizing industrial hemp (*Cannabis sativa* L.) by-products: cannabidiol enrichment in the inflorescence essential oil optimizing sample pre-treatment prior to distillation. Ind. Crops Prod. 128, 581–589. https://doi.org/10.1016/j.indcrop.2018.10.045.

Fiorini, D., Scortichini, S., Bonacucina, G., Greco, N.G., Mazzara, E., Petrelli, R., Torresi, J., Maggi, F., Cespi, M., 2020. Cannabidiol-enriched hemp essential oil obtained by an optimized microwave-assisted extraction using a central composite design. Ind. Crops Prod. 154, 112688. https://doi.org/10.1016/j.indcrop.2020.112688.

Gugliuzzo, A., Francardi, V., Simoni, S., Roversi, P.F., Ferrati, M., Spinozzi, E., Perinelli, D.R., Bonacucina, G., Maggi, F., Tortorici, S., Tropea Garzia, G., Biondi, A., Rizzo, R., 2023. Role of plant essential oil nanoemulsions on host colonization by the invasive ambrosia beetle *Xylosandrus compactus*. Ind. Crops Prod. 195, 116437. https://doi.org/10.1016/j.indcrop.2023.116437.

Gunjevic, V., Grillo, G., Carnaroglio, D., Binello, A., Barge, A., Cravotto, G., 2021. Selective recovery of terpenes, polyphenols and cannabinoids from *Cannabis sativa* L. inflorescences under microwaves. Ind. Crop. Prod. 162, 113247. https://doi.org/10.1016/j.indcrop.2021.113247.

Izzo, L., Castaldo, L., Narváez, A., Graziani, G., Gaspari, A., Rodríguez-Carrasco, Y., Ritieni, A., 2020. Analysis of phenolic compounds in commercial *Cannabis sativa* L. Inflorescences using UHPLC-Q-Orbitrap HRMS. Molecules 25, 631. https://doi.org/10.3390/molecules25030631.

Jokić, S., Jerković, I., Pavić, V., Aladić, K., Molnar, M., Kovač, M.J., Vladimir-Knežević, S., 2022. Terpenes and cannabinoids in supercritical CO_2 extracts of industrial hemp inflorescences: optimization of extraction, antiradical and antibacterial activity. Pharmaceuticals 15, 1117. https://doi.org/10.3390/ph15091117.

Kavallieratos, N.G., Boukouvala, M.C., Ntalli, N., Skourti, A., Karagianni, E.S., Nika, E.P., Kontodimas, D.C., Cappellacci, L., Petrelli, R., Cianfaglione, K., Morshedloo, M.R., Tapondjou, L.A., Rakotosaona, R., Maggi, F., Benelli, G., 2020. Effectiveness of eight essential oils against two key stored-product beetles, *Prostephanus truncatus* (Horn) and *Trogoderma granarium* Everts. Food Chem. Toxicol. 139, 111255. https://doi.org/10.1016/j.fct.2020.111255.

Kitrytė, V., Bagdonaitė, D., Venskutonis, P.R., 2018. Biorefining of industrial hemp (*Cannabis sativa* L.) threshing residues into cannabinoid and antioxidant fractions by supercritical carbon dioxide, pressurized liquid and enzyme-assisted extractions. Food Chem. 267, 420–429. https://doi.org/10.1016/j.foodchem.2017.09.080.

Laws III, J.S., Smid, S.D., 2022. Evaluating *Cannabis sativa* L.'s neuroprotection potential: from bench to bedside. Phytomedicine 107, 154485. https://doi.org/10.1016/j.phymed.2022.154485.

Lewis, G.A., Mathieu, D., Phan-Tan-Luu, R., Mathieu, D., Phan-Tan-Luu, R., 1999. Factor influence studies. Pharmaceutical Experimental Design; Marcel Dekker, Inc.: New York, NY, USA.

Mazzara, E., Carletti, R., Petrelli, R., Mustafa, A.M., Caprioli, G., Fiorini, D., Scortichini, S., Dall'Acqua, S., Sut, S., Nunez, S., Lopez, V., Zheljazkov, V.D., Bonacucina, G., Maggi, F., Cespi, M., 2022b. Green extraction of hemp (*Cannabis sativa* L.) using microwave method for recovery of three valuable fractions (essential oil, phenolic compounds and cannabinoids): a central composite design optimization study. J. Sci. Food Agric. 102, 6220–6235. https://doi.org/10.1002/jsfa.11971.

Mazzara, E., Petrelli, R., Torresi, J., Ricciardi, R., Benelli, G., Maggi, F., 2023. Hemp essential oil: An innovative product with potential industrial applications. In Current Applications, Approaches, and Potential Perspectives for Hemp. Academic Press, pp. 201–279. https://doi.org/10.1016/B978-0-323-89867-6.00012-3.

Mazzara, E., Torresi, J., Fico, G., Papini, A., Kulbaka, N., Dall'Acqua, S., Sut, S., Garzoli, S., Mustafa, A.M., Cappellacci, L., Fiorini, D., Maggi, F., Giuliani, C., Petrelli, R., 2022a. A comprehensive phytochemical analysis of terpenes, polyphenols and cannabinoids, and micromorphological characterization of 9 commercial varieties of *Cannabis sativa* L. Plants 11, 891. https://doi.org/10.3390/plants11070891.

Nuutinen, T., 2018. Medicinal properties of terpenes found in *Cannabis sativa* and *Humulus lupulus*. Eur. J. Med. Chem. 157, 198–228. https://doi.org/10.1016/j.ejmech.2018.07.076.

Palmieri, S., Maggi, F., Pellegrini, M., Ricci, A., Serio, A., Paparella, A., Lo Sterzo, C., 2021. Effect of the distillation time on the chemical composition, antioxidant potential and antimicrobial activity of essential3 oils from different *Cannabis sativa* L. cultivars. Molecules 26, 4770. https://doi.org/10.3390/molecules26164770.

Pieracci, Y., Ascrizzi, R., Terreni, V., Pistelli, L., Flamini, G., Bassolino, L., Fulvio, F., Paris, R., 2021. Essential oil of *Cannabis sativa* L: comparison of yield and chemical composition of 11 hemp genotypes. Molecules 26, 4080. https://doi.org/10.3390/molecules26134080.

Pignatti, S., 1982. Flora d'Italia, Bologna, Edagricole, Bologna, vol. 1, p. 125. ISBN 88-506-2449-2.

Qamar, S., Torres, Y.J., Parekh, H.S., Falconer, J.R., 2022. Fractional factorial design study for the extraction of cannabinoids from CBD-dominant cannabis flowers by supercritical carbon dioxide. Processes 10, 93. https://doi.org/10.3390/pr10010093.

Rossi, P., Cappelli, A., Marinelli, O., Valzano, M., Pavoni, L., Bonacucina, G., Petrelli, R., Pompei, P., Mazzara, E., Ricci, I., Maggi, F., Nabissi, M., 2020. Mosquitocidal and anti-inflammatory properties of the essential oils obtained from monoecious, male, and female inflorescences of hemp (*Cannabis sativa* L.) and their encapsulation in nanoemulsions. Molecules 25, 3451. https://doi.org/10.3390/molecules25153451.

Schober, P., Boer, C., Schwarte, L.A., 2018. Correlation coefficients: appropriate use and interpretation. Anesth. Analg. 126, 1763–1768. https://doi.org/10.1213/ANE.0000000000002864.

Schwarz, A.M., Keresztes, A., Bui, T., Hecksel, R.J., Peña, A., Lent, B., Gao, Z.-G., Gamez-Rivera, M., Seekins, C.A., Chou, K., Appel, T.L., Jacobson, K.A., Al-Obeidi, F.A., Streicher, J.M., 2023. Terpenes from *Cannabis sativa* Induce Antinociception in Mouse Chronic Neuropathic Pain via Activation of Spinal Cord Adenosine A2A Receptors. bioRxiv. https://doi.org/10.1097/j.pain.0000000000003265.

Stanoeva, J.P., Stefova, M., Andonovska, K.B., Stafilov, T., 2017. LC/DAD/MS n and ICP-AES assay and correlations between phenolic compounds and toxic metals in endemic *Thymus alsarensis* from the Thallium Enriched Allchar Locality, 1934578X1701200206 Nat. Prod. Comm. 12. https://doi.org/10.1177/1934578X170120020.

Struik, P.C., Amaducci, S., Bullard, M.J., Stutterheim, N.C., Venturi, G., Cromack, H.T.H., 2000. Agronomy of fibre hemp (*Cannabis sativa* L. Europe. Ind. Crops Prod. 11, 107–118. https://doi.org/10.1016/S0926-6690(99)00048-5.

Tabari, M.A., Khodashenas, A., Jafari, M., Petrelli, R., Cappellacci, L., Nabissi, M., Maggi, F., Pavela, R., Youssefi, M.R., 2020. Acaricidal properties of hemp (*Cannabis sativa* L.) essential oil against *Dermanyssus gallinae* and *Hyalomma dromedarii*. Ind. Crops Prod. 147, 112238. https://doi.org/10.1016/j.indcrop.2020.112238.

Tahir, N.I., Shaari, K., Abas, F., Parveez, G.K.A., Ishak, Z., Ramli, U.S., 2012. Characterization of apigenin and luteolin derivatives from oil palm (*Elaeis guineensis* Jacq.) leaf using LC–ESI-MS/MS. J. Agric. Food Chem. 60, 11201–11210. https://doi.org/10.1021/jf303267e.

Van Den Dool, H., Kratz, P.D., 1963. A generalization of the retention index system including linear temperature programmed gas-liquid parttion chromatography. J. Chromatogr. 11, 463.

Zain, M.S.C., Lee, S.Y., Sarian, M.N., Fakurazi, S., Shaari, K., 2020. In vitro wound healing potential of flavonoid c-glycosides from oil palm (*Elaeis guineensis* Jacq.) leaves on 3t3 fibroblast cells. Antioxidants 9, 326. https://doi.org/10.3390/antiox9040326.

Zheljazkov, V.D., Maggi, F., 2021. Valorization of CBD-hemp through distillation to provide essential oil and improved cannabinoids profile. Sci. Rep. 11, 19890. https://doi.org/10.1038/s41598-021-99335-4.

Zheljazkov, V.D., Noller, J.S., Maggi, F., Dale, R., 2022. Terpenes and cannabinoids yields and profile from direct-seeded and transplanted CBD-*Cannabis sativa*. J. Agric. Food Chem. 70, 10417–10428. https://doi.org/10.1021/acs.jafc.1c06912.

Zheljazkov, V.D., Sikora, V., Dincheva, I., Kačániová, M., Astatkie, T., Semerdjieva, I.B., Latkovic, D., 2020b. Industrial, CBD, and wild hemp: how different are their essential oil profile and antimicrobial activity? Molecules 25, 4631. https://doi.org/10.3390/molecules25204631.

Zheljazkov, V.D., Sikora, V., Semerdjieva, I.B., Kačániová, M., Astatkie, T., Dincheva, I., 2020a. Grinding and fractionation during distillation alter hemp essential oil profile and its antimicrobial activity. Molecules 25, 3943. https://doi.org/10.3390/molecules25173943.